



## RESEARCH ARTICLE

## Corrosion Protection of Tin in 1M HCl by Expired Novacid Drug-Part I

E. M. Attia, N. S. Hassan and A. M. Hyba

Chemistry Department, Faculty of Science (Girls), Al-Azhar University, Nasr city, Cairo, Egypt.

**Manuscript Info****Manuscript History:**

Received: 14 December 2015  
 Final Accepted: 29 January 2016  
 Published Online: February 2016

**Key words:**

Expired drug, Tin, Corrosion,  
 Inhibitor, Polarization.

**\*Corresponding Author**

E. M. Attia.

**Abstract**

Expired Novacid drug (END) in different concentrations (0-9% (v/v)) was examined as corrosion inhibitor for tin electrode in 1M HCl at different temperatures (20 – 60 °C) using weight loss and potentiodynamic techniques. The morphology of the surface was analyzed by scanning electron microscope (SEM) and energy dispersive X-ray (EDS) analysis. Weight loss measurements illustrated that the inhibition efficiency increased with increasing END concentration and solution temperature. Also, adsorption as well as the inhibition process followed first-order kinetics at all concentrations and temperatures. Potentiodynamic measurements showed that END is a cathodic type inhibitor and the adsorption process was chemisorption type and obey Temkin's adsorption isotherm at all concentrations and temperatures studied. Activation energy ( $E_a$ ), enthalpy ( $\Delta H_{ads}^\circ$ ), entropy ( $\Delta S_{ads}^\circ$ ) and free energy of adsorption ( $\Delta G_{ads}^\circ$ ) were calculated and discussed. Results obtained from weight loss and potentiodynamic measurements were in good harmony and confirmed that END is a good corrosion inhibitor for tin in 1M HCl solution.

Copy Right, IJAR, 2016.. All rights reserved.

**Introduction:-**

Tin is a slightly active metal, characterized by its low melting point (231.93 °C), low tensile strength (15 MPa), malleability and good resistance to corrosion. Owing to these properties, this metal is very suitable in many important industrial applications such as the production of soft solders, bronze, and dental amalgam (Mohran *et al.*, 2009). Other properties that have influenced the selection of tin for particular purposes are the low toxicity of tin salts which permit the use of tin in food-grade applications and the absence of catalytic promotion of oxidation processes that may cause changes in oils or other neutral media affecting their quality or producing corrosive acids (Lyon, 2010).

Acid solutions are widely used in industries such as pickling, cleaning, descaling etc., which generally lead to serious metallic corrosion. Tin corrode in acid solutions, evolving hydrogen gas (Lyon, 2010). So it is very important to add corrosion inhibitors to decrease the corrosion rate of the metal. Organic corrosion inhibitors are useful when their addition in small amounts prevents corrosion. At higher concentrations of organic compounds an additional testing for environmental impact is required (Bockris and Reddy, 2000 and Fouda *et al.*, 2015). Most of the well-known acid inhibitors are organic compounds containing nitrogen, sulphur and oxygen atoms (Sharma *et al.*, 2015; Zhu *et al.*, 2016; Zhang *et al.*, 2016 and Siğircik *et al.*, 2016). However, great numbers of cheap drugs are known to possess most of these qualities. But with exposure to physical, chemical or microbiological variables like temperature, pressure, humidity, light or bacteria these drugs became unsuitable for use and became expired (Attia, 2015).

Therefore, the aim of the present research is to study the inhibitive effect of expired Novacid drug (END) on the corrosion of tin in 1M HCl solution using chemical and electrochemical methods at different temperatures.

## Experimental details:-

### Electrode preparation:-

Cylindrical specimen was taken from a rod of tin with the chemical composition (wt %): 97.5 Sn; 0.78 Ti; 0.4 Si and 0.013 Fe. The rod was mounted in a glass tube of appropriate diameter using epoxy resin leaving a specified circular surface area ( $2.27 \text{ cm}^2$ ) to contact the electrolyte. For weight loss measurements, the rod was cut into several coupons; each one has a surface area  $5.875 \text{ cm}^2$ . The surface of tin electrode was polished with emery papers ranging from 600 to 1200 grit, cleaned in distilled water, degreased in ethanol and finally dried. The tin electrode used in this work was provided by the General Company for Metal gamet (Helwan).

### Solutions and inhibitor:-

Novacid (Syrup) is an Egyptian drug produced by Chemical Industries Development (CID). It is an analgesic, antipyretic and spasmolytic. In this study, it was tested as a corrosion inhibitor and the concentration of the solution was expressed in terms of % (v/v). Each 100 ml of Syrup contains 5g of metamizole as reported in the pamphlet of drug. The empirical formula of metamizole, the active ingredient of Novacid Syrup, is  $\text{C}_{13}\text{H}_{17}\text{N}_3\text{O}_4\text{S}$ , with molecular weight being  $311.357 \text{ g/mol}$  and melting point being  $187^\circ\text{C}$ . The chemical name of metamizole is Sodium [(1,5-dimethyl-3-oxo-2-phenyl-2,3-dihydro-1H-pyrazol-4-yl)(methyl)amino]methanesulfonate hydrate (1:1:1) and its molecular structure is represented in Figure 1. Different concentrations (1, 3, 5, 7 and 9 %) of expired Novacid drug (END) were prepared by diluting a known volume of drug in appropriate volume of 1M HCl solution. The 1M HCl solution was prepared using reagent grade concentrated acid and bi-distilled water.

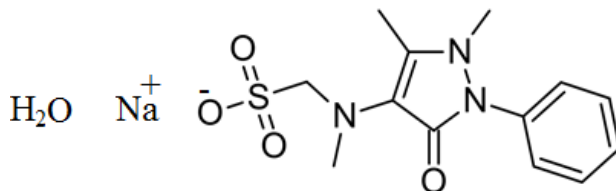


Fig 1: Molecular structure of metamizole.

## Experimental Methods

### a) Weight loss measurements:-

Weight loss measurements were carried out in a 25 ml glass beaker placed in a water bath with thermostat control. The tin coupons had a cylindrical shape of 1.7 cm diameter and 0.25 cm thickness. The coupons were successively polished with emery papers, degreased in ethanol, washed in doubly distilled water, dried, and finally weighted in analytical balance Model FA 2104A (cap.: 210 g, d.: 0.1mg). The weighted coupons are suspended in 25 ml 1M HCl solutions in absence and presence of different concentrations of END at different temperatures ( $20, 30, 40, 50$  and  $60^\circ\text{C}$ ). After passing the specified immersion time, each coupon was withdrawn from the test solution, dried in moisture-free desiccator and re-weighted. In each case, the difference in weight was taken as the weight loss. The corrosion rate was calculated according to Eq. 1 (Karthik *et al.*, 2015):

$$C_R = (\Delta W \times 534) / Atd \quad (1)$$

where  $C_R$  is the corrosion rate (mpy),  $\Delta W$  (g) is the difference in the coupons weight before and after immersion in the tested solution,  $A$  is the surface area of the tin coupons ( $\text{cm}^2$ ),  $t$  is the exposure time (h) and  $d$  is density of metal in  $\text{g/cm}^3$ . The degree of surface coverage ( $\theta$ ) was calculated using Eq. 2:

$$\theta = \frac{W_o - W_i}{W_o} \quad (2)$$

where  $W_i$  and  $W_o$  are the values of weight losses of tin coupons in inhibited and uninhibited solutions, respectively. The inhibition efficiency  $IE\%$  was calculated according to Eq. 3:

$$IE\% = \theta \times 100 \quad (3)$$

### b) Potentiodynamic polarization measurements:-

Potentiodynamic polarization measurements were generated using an Electronic Potentiostat Wenking (Model POS 73). The measurements were performed with the aid of a glass cell (25 ml solution) containing three openings for electrodes. A saturated calomel electrode (SCE) provided with a Luggin capillary probe and a platinum sheet ( $2 \text{ cm}^2$ ) were used as the reference and the auxiliary electrodes, respectively. The  $E - \log I$  curves for all solutions were swept from  $-2000 \text{ mV(SCE)}$  to  $+2000 \text{ mV(SCE)}$  at scan rate  $2 \text{ mVs}^{-1}$ . The working electrode was first immersed into the test solution for 150 min to reach a quasi-stationary value of the open circuit potential prior to the measurements.

The corrosion rate ( $C_R$ ) in mpy, was calculated using Eq.4(Pathak, 2013):

$$C_R = 0.13 \times I_{\text{corr}} \times e/d \quad (4)$$

where 0.13 is the metric and time conversion factor,  $I_{\text{corr}}$  is the corrosion current density in  $\mu\text{A}/\text{cm}^2$ ,  $e$  and  $d$  are the equivalent weight and density of metal in  $\text{geq}/\text{mol}$  and  $\text{g}/\text{cm}^3$  respectively. Values of  $I_{\text{corr}}$  and corrosion potential ( $E_{\text{corr}}$ ) were evaluated from intersection of the linear anodic and cathodic branches of Tafel plots and were calculated in absence and presence of different concentrations of END. Each experiment was repeated three times at least. Degrees of surface coverage ( $\theta$ ) in potentiodynamic measurements were calculated using Eq. 5.

$$\theta = \left[ 1 - \frac{I_{\text{corr}}}{I_{\text{corr}}^0} \right] \quad (5)$$

where  $I_{\text{corr}}^0$  and  $I_{\text{corr}}$  are the corrosion current densities in absence and presence of END, respectively.

### Surface characterization:-

After exposure to 1M HCl in the absence and presence of END (1- 9%) for 2h immersion, the surface morphologies of tin coupons were examined by scanning electron microscopy (SEM) and energy dispersive X-ray analysis (EDS). The immersions for surface analysis were carried out at 20 and 60 °C.

## Results and discussion:-

### Weight loss measurements

#### a) Effect of immersion time:-

Figure 2-a illustrated the weight loss ( $\text{mg}/\text{cm}^2$ ) of tin electrode in 1M HCl in absence and presence of different concentrations (1-9%) of END at various time intervals which operate at 20 °C. The present results indicated that weight losses of tin in presence of END were lower than that of free HCl (0%) solution. It increased and varied linearly with time for all concentrations. The obtained linearity indicated the absence of insoluble surface film during corrosion. In addition the inhibitor was first adsorbed onto the metal surface and, therefore, impedes the corrosion process (Lokesh *et al.*, 2014). These results led to the conclusion that END is fairly efficient as inhibitor for tin dissolution in 1M HCl solution. The same behaviour was observed at the temperature range 30 – 60 °C.

Figure 2-b illustrated that corrosion rate of tin in free HCl was high and increased with increasing exposure time. Moreover, tin would dissolve as  $\text{Sn}^{2+}$  ions at  $\text{pH} < 2$  (Lyon, 2010). In presence of END, the corrosion rates became low and decreased with time at low inhibitor concentrations (1 and 3%). At higher concentrations (5, 7 and 9%), the corrosion rates had little observable changed values after prolonged time. The shape of the curves in the first 45 min indicated the passivation of tin by formation of a film that consists of  $\text{Sn}(\text{OH})_4$ . With increasing time, the hydroxide transformed gradually to tin (IV) oxide,  $\text{SnO}_2$ , which was more stable at a lower pH (Lyon, 2010). This was illustrated by the stable part of the curves which constituted the period from 45 to 120 min.

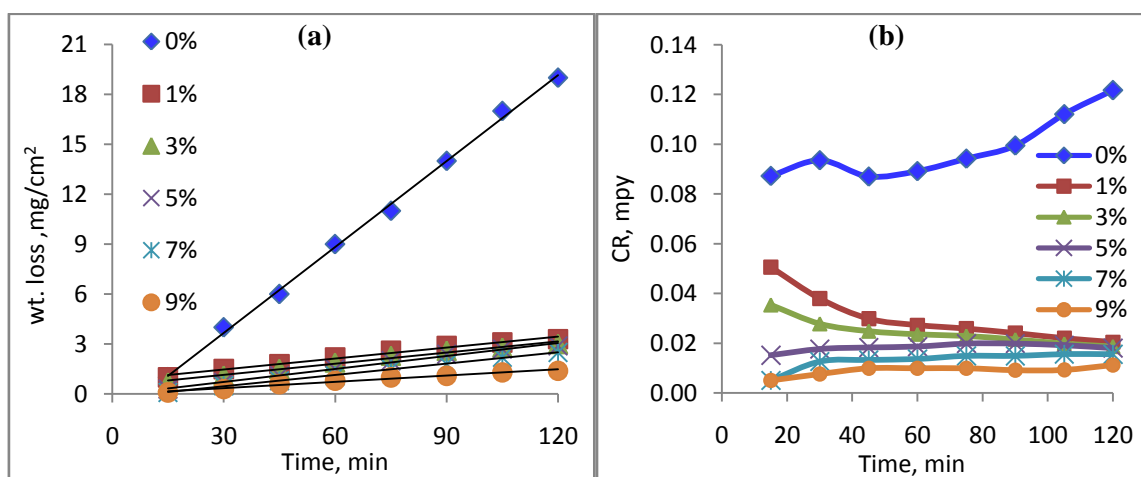


Fig 2: Variation in weight loss (a) and corrosion rates (b), with exposure time for corrosion of Sn in 1M HCl in absence and presence of different concentrations of END at 20 °C.

**b) Effect of inhibitor concentration:-**

The corrosion rates and inhibition efficiencies of tin at different concentrations (0-9%) of END in 1M HCl are summarized in Table 1. The inhibition efficiency increased while the corrosion rate decreased as the concentration of inhibitor increased from 1 to 9% (v/v). This behavior was observed at all temperatures studied. The change of IE% and  $C_R$  might be resulted from the increased adsorption and coverage of inhibitor on the tin surface with increasing inhibitor concentration. The change of IE% values with concentrations in Table 1 revealed that END was concentration-dependent inhibitor. It was postulated that the extremely low corrosion rates in presence of inhibitor compared with that in free solution were due to the presence of a thin, stable passive film that formed on the metal surface (Fouda *et al.*, 2015).

**Table 1: Corrosion rates (mpy) and inhibition efficiency (IE %) values for tin corrosion in 1M HCl in absence and presence of different concentrations of END at different temperatures**

Conc. %	20 °C		30 °C		40 °C		50 °C		60 °C	
	$C_R$	IE%								
0	0.1217	-	0.1834	-	0.2378	-	0.2984	-	0.3797	-
1	0.0205	83.14	0.0242	86.78	0.0273	88.49	0.0286	90.42	0.0305	91.98
3	0.0186	84.67	0.0236	87.12	0.0261	89.02	0.0273	90.83	0.0298	92.14
5	0.0180	85.18	0.0186	89.83	0.0236	90.06	0.0255	91.46	0.0279	92.63
7	0.0155	87.23	0.0180	90.17	0.0224	90.59	0.0230	92.29	0.0255	93.29
9	0.0112	90.80	0.0168	90.85	0.0174	92.68	0.0186	93.75	0.0230	93.94

**c) Effect of Temperature:-**

Corrosion rates increased with increasing temperature in both uninhibited and inhibited solutions. However it went up more rapidly in the absence of inhibitor (Table 1). These results confirmed that END acted as an effective inhibitor in the studied temperature range. Also, it was noted that the inhibition efficiency depended on the temperature and increased with the rise of temperature from 20 °C to 60 °C. The inhibition efficiency reached its maximum value (93.94) at 9% of inhibitor when the temperature reached to 60 °C which suggested chemical adsorption mechanism and represented excellent inhibitive ability of END.

**d) Kinetics of Corrosion Inhibition:-**

The kinetics of the system was proposed by converting the weight loss ( $\text{mgcm}^{-2}$ ) to concentration (g/l) of the corrodent tin, and later converted to molar concentrations in mol/l. Assuming  $a$  (mol/l) is the initial concentration of the tin electrode and  $x$  (mol/l) is the final concentration of tin had decomposed into corrosion products after time  $t$ . Therefore, the corrodent concentration of tin at time  $t$  is  $a - x$  (mol/l) (Sharma and Sharma, 2008). A plot of  $\log(a - x)$  or  $\log[\text{Sn}]$  vs. time (at 20 °C) showed straight line graphs with regression coefficient ( $R^2$ ) values almost equal to unity, confirming a first order kinetics (Figure 3). In a similar study Attia (2015) applied  $\log[\text{corrodent}]$  and used the following rate equation:

$$-\log[\text{corrodent}] = K_1 t/2.303 \quad (6)$$

where  $K_1$  is the first order rate constant and  $t$  is the time in minutes. Also, the half- life of a first order reaction is related to the rate constant according to Eq. 7 (Atkins and Paula, 2014):

$$t_{0.5} = \frac{0.963}{K_1} \quad (7)$$

Values of rate constants and half-lives calculated from the slopes of the kinetic plots at temperature range 20 – 60 °C for tin electrode in free 1M HCl was tabulated in Table 2. The results revealed that the first order corrosion rate constants ( $K_1$ ) increased while the half-lives of corrosion rates ( $t_{0.5}$ ) decreased with increasing of temperature. This indicated increasing of tin corrosion with temperature rising in free 1M HCl solution.

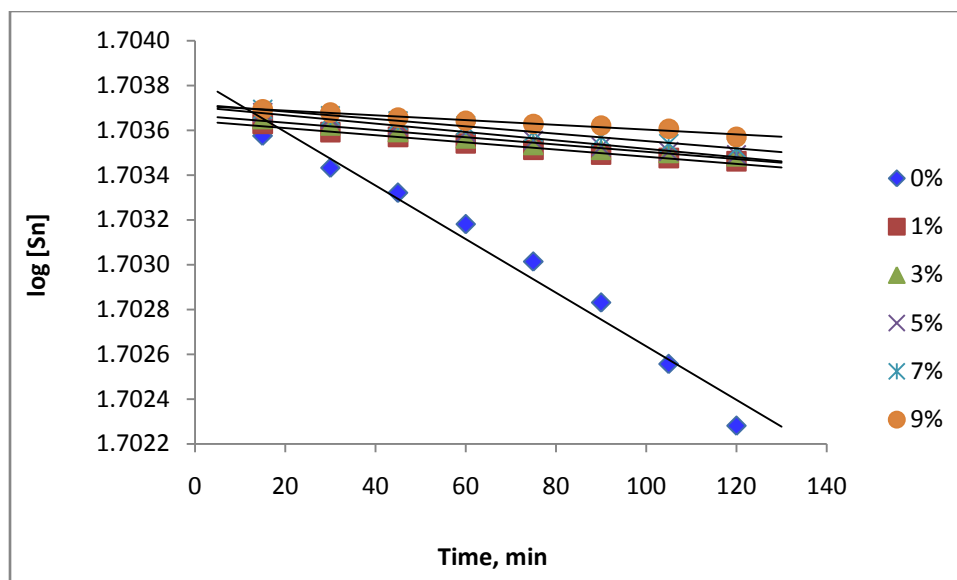


Fig 3: kinetic plots for the corrosion of Sn in absence and presence of different concentrations of END at 20 °C.

**Table 2: Kinetic parameters for the corrosion of tin in free 1M HCl at different temperatures**

Temp. °C	$K_1 \text{ min}^{-1}$	$t_{0.5} \text{ min}$
20	2.30E-05	3.01E+04
30	4.61E-05	1.50E+04
40	4.61E-05	1.50E+04
50	6.91E-05	1.00E+04
60	9.21E-05	7.52E+03

As a general trend, addition of END to the corrosive 1M HCl solution decreased the rate constant and increased the half-lives of corrosion reactions. On the other hand, increasing of temperature or inhibitor concentration had no considerable effect on the rate constants or half-lives of corrosion reactions. The corrosion rate constants ( $K_1$ ) for most of concentrations equaled to  $4.61\text{E}-06 \text{ min}^{-1}$  and the half-lives of corrosion reactions equaled to  $1.50\text{E}+05 \text{ min}$ . An exception was observed for 9% END at 20 °C and 5% at 30 °C which both gave  $K_1 = 2.30\text{E}-06$  and  $t_{0.5} = 3.01\text{E}+05$ . The chemistry behind this behavior was not understandable.

#### e) SEM- EDS analysis:-

Figure 4-a showed the surface morphology of tin coupons before treatment with HCl solution, which in general seemed smooth with only some nickeds. After 2 h exposure to 1M HCl free from END, at 20 °C, the tin surface became rough and porous due to many corrosion products which constituted inhomogeneous and imperfect film (Figure 4-b). The disappearance of the original nickeds was evidence of anodic dissolution of Sn. After addition of 1% END to corrosive solution, it was clear that the surface was subjected to corrosion inhibition where the corrosion products decreased (Figure 4-c). However the surface still inhomogeneous and a lot of defects were presented suggesting the poor corrosion protection performance at 1% END. At 3% END, the corrosion products produced a net like surface film with a large population of surface holes (Figure 4-d). The surface had appeared spongy at 5% END with little surface defects (Figure 4-e). More pronouncedly was the change in the shape and surface features of the film on the tin electrode after increasing the inhibitor concentration to 7% (Figure 4-f). The film had lost its spongy nature and became ragged while the surface had appeared wavy at 9% END (Figure 4-g). At this concentration, the corrosion products disappeared and the produced films became homogenous and perfect with good protective performance for tin electrode. This led to smoother metal surface and the flawed regions were repaired. Figure 4-h illustrated that the protective film formed at 60 °C in 9% END solution was more compact and had less defects compared with that formed at 20 °C (Figure 4-g). This finding indicated that the protective properties of the formed films were better at higher temperatures.

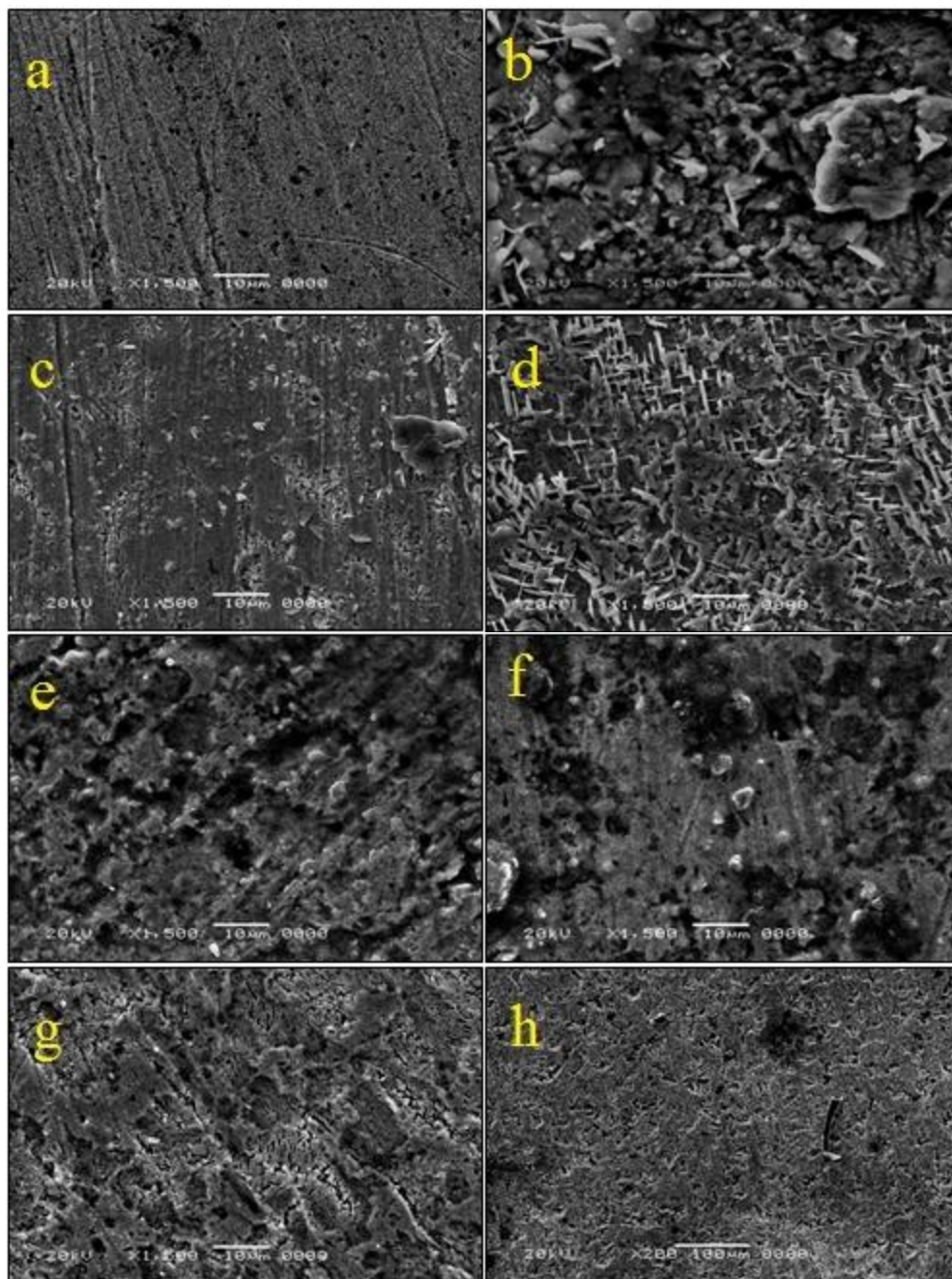


Fig 4: SEM micrograph for Sn coupons, a: abraded Sn electrode; b: Sn in free HCl at 20 °C; c, d, e, f and g: Sn in 1, 3, 5, 7 and 9% END at 20 °C respectively; h: Sn in 9% END at 60 °C.

As determined by EDS analysis, it was seen that abraded tin contained only the elements of rod composition. Very low amount of oxygen was detected on the Sn surface in free HCl solution, this excluded the possibility of formation of any oxide layer on the Sn surface (Figures 5 and 6). Table 3 illustrated the amount of elements, detected by EDS analysis, on the tin surface before and after addition of different concentrations of END to 1M HCl solution. Analysis of data indicated that the oxygen content of the surface was obviously increased to 29.3 at 1 and 5 % END but this percent was still less than the amount required to form the stoichiometry of minimum tin oxide. EDS analysis showed a high oxygen content of 53.127 at 3% END, giving an O/Sn ratio of approximately 1:1, the stoichiometry of SnO. At 9% END the oxygen content reached to 73.127 which exceeded the stoichiometry of SnO<sub>2</sub>.

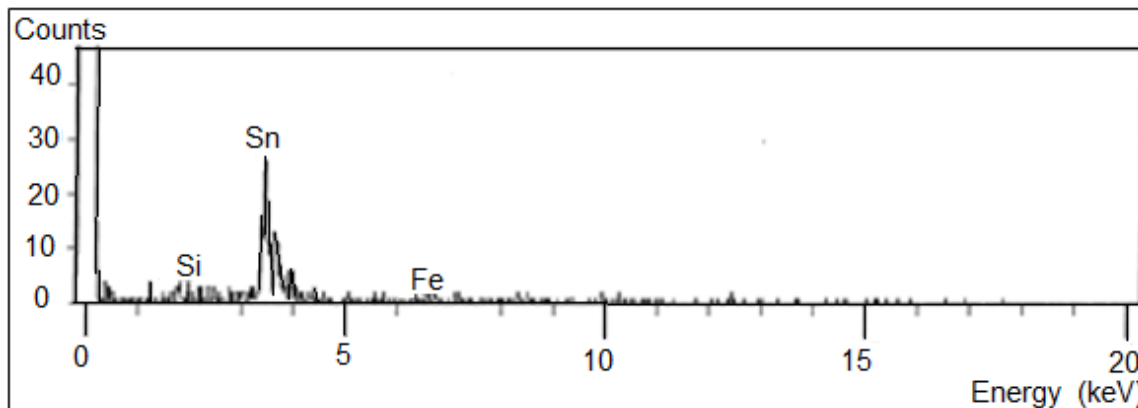


Fig 5: EDS analysis of abraded Sn before immersion in HCl solution.

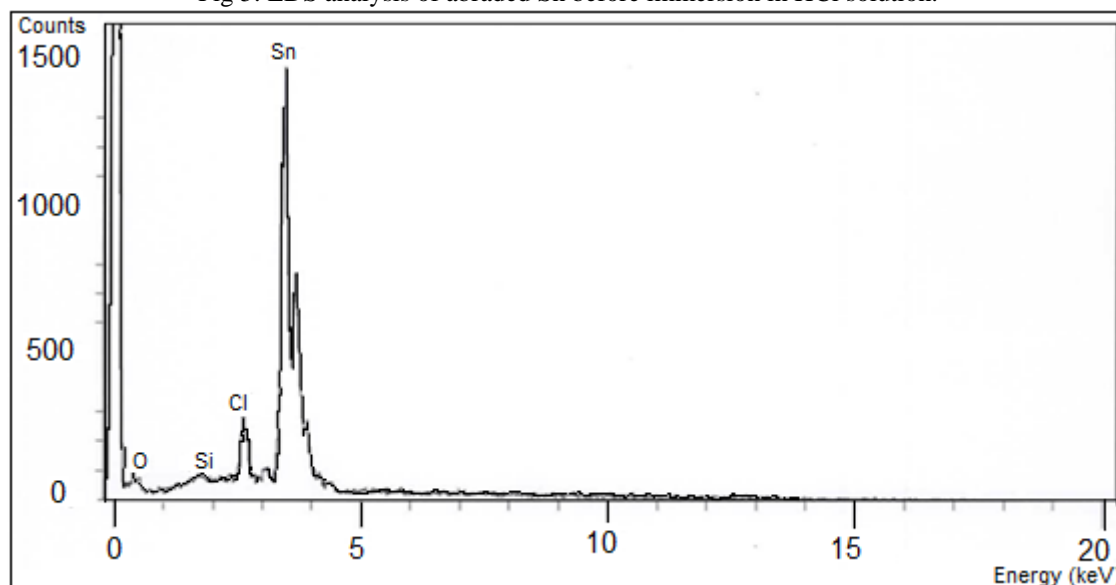


Fig 6: EDS analysis of Sn after immersion in free 1M HCl solution.

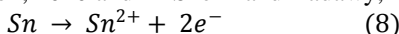
**Table 3: Elemental analysis of tin surface after immersion for 2 h in 1M HCl in absence and presence of different concentrations of END**

$C_{inh}$ , %	Sn	O	Cl	Si	Ti	S	Fe
0	90.703	5.433	3.510	0.357	-	-	-
1	69.887	29.327	0.423	0.393	0.033	-	-
3	41.220	53.127	5.360	0.120	0.180	-	-
5	66.590	29.357	2.190	1.023	-	0.620	0.218
7	72.727	19.747	4.077	0.483	-	2.963	-
9	25.097	73.127	0.483	0.170	0.103	1.020	-

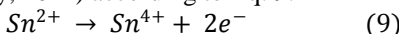
**Potentiodynamic polarization:-****a) Effect of inhibitor concentration:-**

Polarization measurements were carried out in order to gain knowledge concerning the kinetics of the cathodic and anodic reactions. Potentiodynamic polarizations of tin were performed in the temperature range of 20–60 °C in 1M HCl solution in absence and presence of different concentrations of END and the plots were illustrated in Figure 7. The corrosion parameters at different concentrations and temperatures were listed in Table 4. Addition of END to HCl media reduced markedly the current density in the cathodic branch of the potentiodynamic polarization curves in comparison with that in the free solution (Figure 7).

At potentials just above its reversible value, tin dissolves under anodic polarization in acids initially as stannous ion ( $Sn^{2+}$ ) (Abd El-Rehim *et al.*, 2004; Lyon, 2010 and El-Sherif and Badawy, 2011) according to Eq. 8.



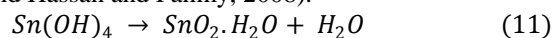
The stannous ion is unstable in water at most values of pH (except in acid concentrations typically  $>1M$ ), while at low concentrations, it is hydrolyzed forming a number of species, depending on pH:  $SnOH^{+}$ ,  $Sn(OH)_2$ ,  $Sn(OH)_3^{-}$ , etc. (Lyon, 2010). Accordingly at more anodic potentials, the  $Sn^{2+}$  species easily oxidize to the  $Sn^{4+}$  (Hassan and Fahmy, 2008 and El-Sherif and Badawy, 2011) according to Eq. 9:



The  $Sn^{4+}$  species hydrolyze to the hydroxide even in acidic solutions according to Eq. 10 forming the highly insoluble  $Sn(OH)_4$  (Cotton and Wilkinson, 1972 and Smith, 1973)



The dehydration of  $Sn(OH)_4$  to  $SnO_2$  involved a free energy change of about  $-42 \text{ kJ mol}^{-1}$  (Abd El-Rehim *et al.*, 2004). So that, the stability of the passive film increased with its irreversible dehydration to  $SnO_2$  (Smith, 1973; Abd El-Rehim *et al.*, 2004 & 2006 and Hassan and Fahmy, 2008).



In the presence of inhibitor molecules and when the surface was completely covered with  $Sn(OH)_4$  and/or  $SnO_2 \cdot H_2O$  film, the active surface sites on the anode surface would be blocked and the dissolution current felled to a small value, indicating the onset of passivation (El-Sherif and Badawy, 2011 and Hassan and Fahmy, 2008).

According to the values of corrosion potentials ( $E_{corr}$ ) listed in Table 4, cathodic behaviors were observed at all temperatures studied except at  $30 \text{ }^{\circ}\text{C}$ , in which anodic behaviors were observed at lower inhibitor concentrations (1, 3 and 5%) while cathodic behaviors were observed at higher concentrations (7 and 9%). This showed that the effect of inhibitor on the cathodic reaction was more observable than on the anodic reaction (Golestani *et al.*, 2014). Since the changes in  $E_{corr}$  values exceeded  $85 \text{ mV}$  in relation to that measured for free HCl solution, hence, it can be concluded that END could act as cathodic inhibitor (Attia, 2015).

The values of  $I_{corr}$  and  $C_R$  decreased with increasing inhibitor concentration at all temperatures. These decrements indicated that addition of END molecules inhibited the corrosion process by increasing the adsorption of inhibitor and surface coverage ( $\theta$ ) on tin surface parallel with increasing inhibitor concentration. This demonstrated that the inhibition degree depended on the concentration of inhibitor.

The anodic and cathodic Tafel slopes ( $\beta_a$  and  $\beta_c$ ) in presence of different concentrations of END varied greatly from that of free  $1M$  HCl solution. This variation was considered as insisting to control the anodic dissolution of tin and to delay the cathodic hydrogen evolution reaction.

The IE% values showed that the inhibition process was more pronounced with increasing inhibitor concentration. The highest IE% occurred at 9% END concentration, was most likely due to the adsorption and formation of a good protective film. The formation of a protective film was a result of the interaction of inhibitor molecules with atoms of the metal surface (Attia, 2015). The inhibition efficiency (IE%), determined by the two methods (weight loss and potentiodynamic polarization), as a function of concentration of END in  $1M$  HCl were in agreement.

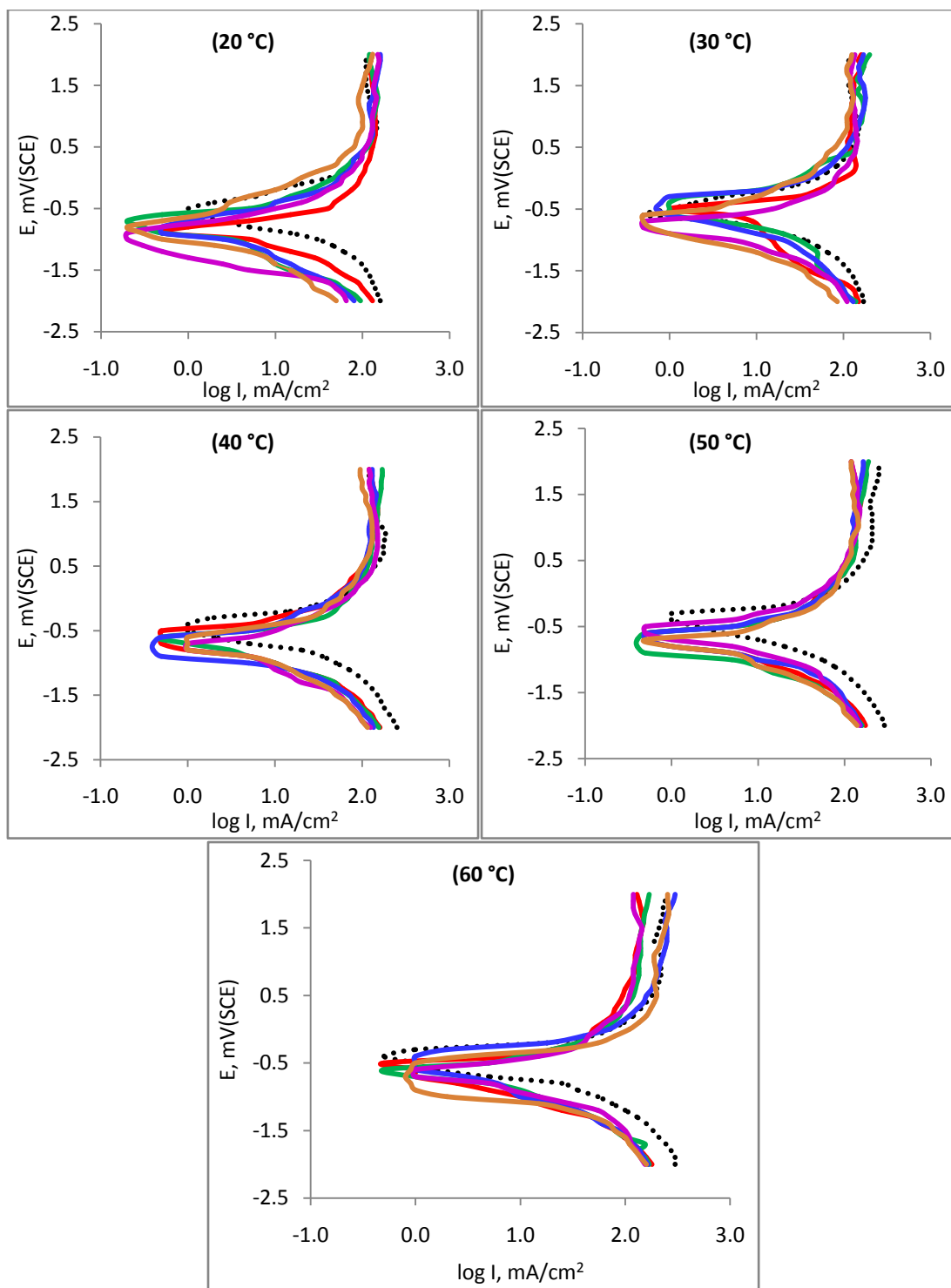


Fig 7: Tafel plots at different temperatures for tin in 1M HCl in absence and presence of different concentrations of END.

**Table 4: Corrosion data for tin at different concentration of END at temperature range 20 – 60 °C**

Temp., °C	Conc., % (v/v)	$E_{corr}$ , mV/SCE	$I_{corr}$ , mA/cm <sup>2</sup>	$C_R$ , mpy	$\beta_a$ , mV/dec	$-\beta_c$ , mV/dec	$\theta$	IE%
20	0	-550	50.1	52903	2000	10000	-	-
	1	-900	9.8	10344	1250	909	0.80446	80.45
	3	-700	7.9	8384	2000	1428	0.84151	84.15
	5	-850	6.3	6660	2000	769	0.87411	87.41
	7	-950	5.0	5290	2500	666	0.90000	90.00
	9	-800	4.5	4750	1666	666	0.91021	91.02
30	0	-600	63.1	66605	1000	1000	-	-
	1	-500	10.0	10555	769	1111	0.84151	84.15
	3	-500	8.7	9183	1000	1250	0.86211	86.21
	5	-500	6.7	7072	1428	909	0.89381	89.38
	7	-750	5.9	6227	909	1000	0.90649	90.65
	9	-700	5.3	5594	1111	1250	0.91600	91.59
40	0	-450	66.1	69740	1428	666	-	-
	1	-600	10.3	10872	1250	1428	0.84410	84.41
	3	-650	9.0	9500	1000	1428	0.86377	86.38
	5	-750	7.0	7388	1250	1000	0.89405	89.40
	7	-750	6.0	6333	1250	769	0.90918	90.92
	9	-700	5.5	5805	1000	1250	0.91675	91.67
50	0	-400	70.8	74733	1666	833	-	-
	1	-650	10.6	11188	1428	1250	0.85028	85.03
	3	-750	8.5	8972	1250	1000	0.87994	87.99
	5	-700	6.5	6861	2500	769	0.90819	90.82
	7	-600	5.5	5805	1250	1666	0.92231	92.23
	9	-750	4.7	4961	1250	1000	0.93361	93.36
60	0	-400	112.2	118433	10000	1250	-	-
	1	-600	13.0	13722	1000	1111	0.88413	88.41
	3	-620	12.0	12666	769	1000	0.89304	89.30
	5	-500	10.0	10555	1000	1250	0.91087	91.09
	7	-650	8.0	8444	1000	1000	0.92869	92.87
	9	-700	6.5	6861	588	909	0.94206	94.21

**b) Effect of temperature:-**

Returning to Table 4, the surface coverage ( $\theta$ ) and inhibition efficiencies (IE%) increased regularly with increasing of temperature for all investigated concentrations where the maximum efficiency was 94.21% at 60 °C for 9% END. Increasing inhibition efficiency with increasing of temperature was attributed to chemical adsorption mode (AL-Sawaad, 2013). Thus, at high degree of coverage, the diffusion through the surface layer (containing the inhibitor and corrosion products) became the rate determining step of the metal dissolution process i.e., the adsorption mode for END was chemisorption mode.

**c) Kinetic and thermodynamic parameters:-**

In order to gain more information about the effectiveness of the studied inhibitor at higher temperatures, an experimental dependence of Arrhenius-type equation on temperature was observed between the corrosion rate and temperature and illustrated in Eq. 12.

$$\log C_R = A - (E_a/2.303 RT) \quad (12)$$

where  $A$  is the extrapolation factor,  $E_a$  is the activation energy,  $R$  is the universal gas constant and  $T$  is the absolute temperature. A plot of  $\log C_R$  vs.  $1/T$  gives straight line with slope  $E_a/2.303 R$  and the intercept is the constant  $A$ . Figure 8 represents the relation between  $\log (C_R)$  and reciprocal of the absolute temperature of tin in 1M HCl solution in absence and presence of investigated END. The values of  $E_a$  are given in Table 5.

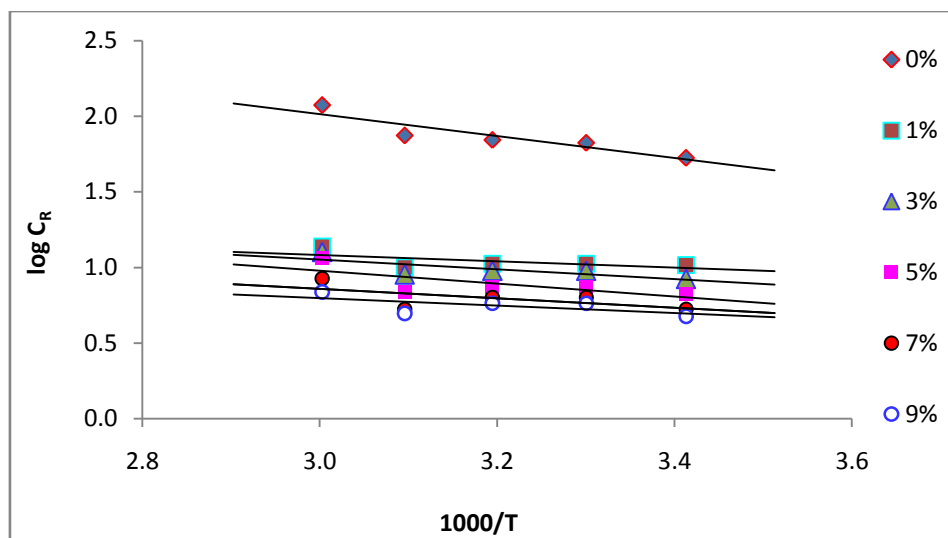


Fig 8: Arrhenius plot for Sn in absence and presence of different END concentrations.

An alternative formulation of Arrhenius equation is the transition state equation (Fouda *et al.*, 2015):

$$\log C_R/T = \log(R/Nh) + (\Delta S^\circ/2.303R) - (\Delta H^\circ/2.303RT) \quad (13)$$

where  $h$  is the Planck's constant,  $N$  is Avogadro's number,  $\Delta S^\circ$  is the entropy change of activation and  $\Delta H^\circ$  is the enthalpy change of activation. Figure 9 showed a plot of  $\log C_R/T$  against  $1/T$ . Straight lines were obtained with a slope of  $(-\Delta H^\circ/2.303R)$  and intercept of  $(\log(R/Nh) + (\Delta S^\circ/2.303R))$  from which the values of  $\Delta H^\circ$  &  $\Delta S^\circ$  were calculated and given in Table 5.

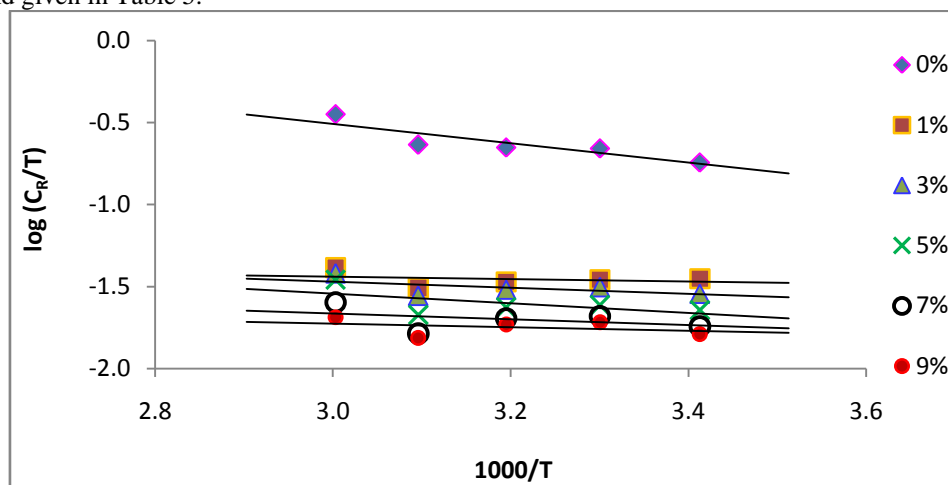


Fig 9: Transition state plot for Sn in absence and presence of different END concentrations.

**Table 5: Kinetic and thermodynamic parameters of tin in 1M HCl in absence and presence of different concentrations of END**

Conc. %	Kinetic parameters			Thermodynamic parameters		
	A	E <sub>a</sub> kJ/mol	R <sup>2</sup>	ΔH <sup>o</sup> kJ/mol	ΔS <sup>o</sup> J/mol K	R <sup>2</sup>
0	4.2	13.9	0.8402	11.3	-173.4	0.7781
1	5.0	21.7	0.9005	19.1	-157.4	0.8760
3	6.7	32.1	0.9603	29.5	-125.8	0.9533
5	7.2	35.4	0.9675	32.8	-116.5	0.9623
7	7.5	37.9	0.9813	35.3	-110.2	0.9784
9	8.0	42.2	0.9747	39.6	-100.0	0.9712

Apparent activation energy ( $E_a$ ) increased with increasing of END concentration indicating the higher protective efficiency. This increase in the apparent activation energy might be understood as chemical adsorption (AL-Sawaad, 2013). On the other hand, the increase in activation energy could be ascribed to significant increase in the adsorption of the inhibitor molecules on the tin surface with increase in temperature (Szauer and Brand, 1981). The significant difference between these values and the value for the free acid (0%) indicated that END retarded the corrosion of tin in HCl solution.

From Table 5 it was clear that the positive values of  $\Delta H^\circ$  in absence and presence of different concentrations of END reflected the endothermic nature of dissolution process which meant that dissolution of tin is difficult. The Table also, showed that the presence of END produced higher values for  $\Delta H^\circ$  than those obtained for the uninhibited solution. This indicated higher protection efficiency. This might be attributed to the presence of an energy barrier for the reaction, that is, the process of adsorption led to a rise in enthalpy of the corrosion process (Ansari *et al.*, 2014 and Fouda *et al.*, 2015). In addition, the values of  $\Delta S^\circ$  were large and negative. This implied that the activated complex in the rate determining step represented association rather than dissociation meaning that a decrease in disordering took place on going from reactants to activated complex and the increase in the system ordering accompanied the dissolution process (Abdel Motaal and AL-Malki, 2009 and Al-Bonayan, 2015).

#### d) Adsorption isotherm

Theoretically, the adsorption process can be regarded as a single substitution process where the inhibitor molecules, in the aqueous solution substitute numbers of water molecules adsorbed on the metal surface (Pardo *et al.*, 2006). The degrees of surface coverage ( $\theta$ ) for different inhibitor concentrations in 1M HCl in the temperature range (20–60 °C) were assessed by Tafel plot. Data were tested graphically by fitting to various isotherms. The best fitting coincide with Temkin adsorption isotherm (Figure 10) that assumed a uniform distribution of adsorption energy which increased with increase of the surface coverage. This model could be represented by Eq. 14 (Ejikeme *et al.*, 2015).

$$\exp(-2a\theta) = K_{ads} C \quad (14)$$

where  $K_{ads}$  is the adsorption equilibrium constant which represents the strength between adsorbate and adsorbent. Values of the parameter ( $a$ ), describe the molecular interaction in the adsorbed layer and consider a measure for the steepness of the adsorption isotherm. It could have both positive and negative values. Rearranging and taking logarithm of both sides of Eq. (14), the Eq. (15) is obtained (Sheeja and Subhashini, 2014).

$$\theta = \frac{-2.303 \log K_{ads}}{2a} - \frac{2.303 \log C}{2a} \quad (15)$$

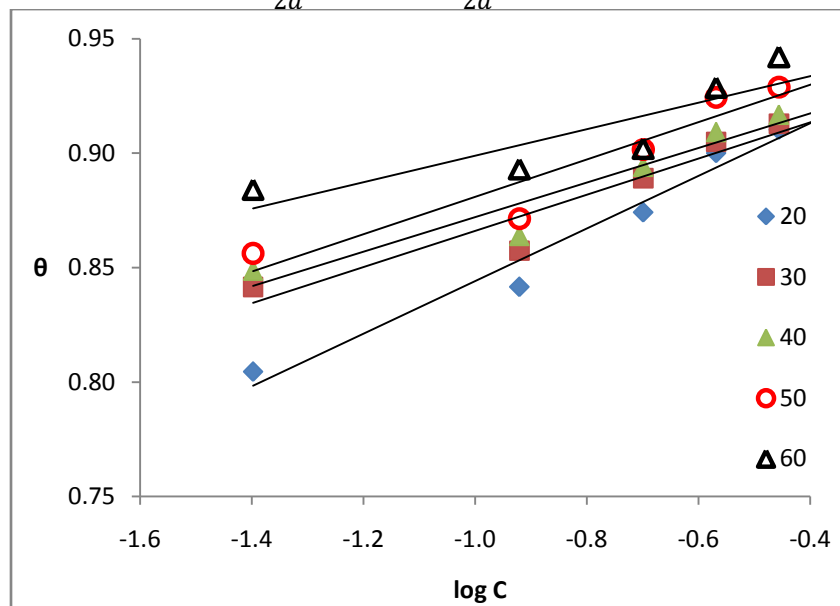


Fig 10: Temkin adsorption isotherm for adsorbed END on tin surface in 1M HCl at different temperatures (20 – 60 °C).

Temkin adsorption parameters were recorded in Table 6. It indicated that the inhibitor obeyed the Temkin model since the experimental data presented adequate straight line fitting for the applied adsorption isotherm.

Thermodynamic parameters are important to further understand the adsorption process of inhibitor on Sn/solution interface. The equilibrium adsorption constant,  $K_{ads}$  is related to the standard Gibb's free energy of adsorption ( $\Delta G_{ads}^{\circ}$ ) with the following equation (Ansari *et al.*, 2014):

$$K_{ads} = (1/55.5) \exp -(\Delta G_{ads}^{\circ}/RT) \quad (16)$$

The standard adsorption enthalpy ( $\Delta H_{ads}^{\circ}$ ) could be calculated on the basis of the following Van't Hoff equation (Ansari *et al.*, 2014):

$$\ln K_{ads} = -\frac{\Delta H_{ads}^{\circ}}{RT} + D \quad (17)$$

where the value of 55.5 is the molar concentration of water in the solution in (mol/l),  $R$  is the universal gas constant,  $T$  is the absolute temperature and  $D$  is integration constant. The standard adsorption enthalpy ( $\Delta H_{ads}^{\circ}$ ) can also be calculated from the Gibbs-Helmholtz equation (Ansari *et al.*, 2014):

$$\frac{\Delta G_{ads}^{\circ}}{T} = \frac{\Delta H_{ads}^{\circ}}{T} + K \quad (18)$$

To calculate the enthalpy of adsorption,  $\ln K_{ads}$  was plotted against  $1/T$  (Figure 11-a) and straight line was obtained with slope equal to  $\Delta H_{ads}^{\circ}/R$ . Also, the variation of  $\Delta G_{ads}^{\circ}/T$  vs.  $1/T$  gives straight line with slope equal to  $\Delta H_{ads}^{\circ}$  (Figure 11-b).

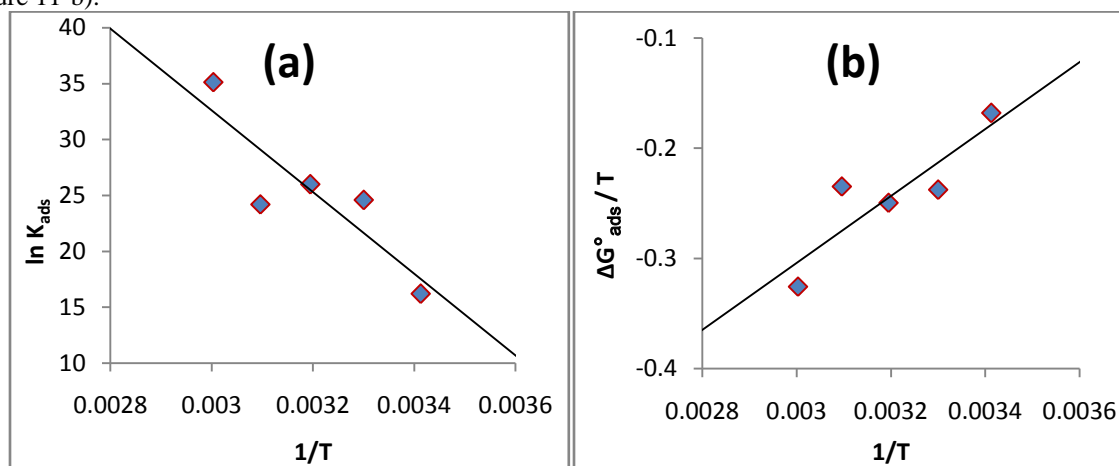


Fig 11: (a) Van't Hoff's plot, (b) Gibbs-Helmholtz's plot.

With the obtained both parameters of  $\Delta G_{ads}^{\circ}$  and  $\Delta H_{ads}^{\circ}$ , the standard adsorption entropy ( $\Delta S_{ads}^{\circ}$ ) can be calculated using Eq. 19 (Arctander, 1969 and Ansari *et al.*, 2014). All the standard thermodynamic parameters are listed in Table 6.

$$\Delta S_{ads}^{\circ} = \frac{\Delta H_{ads}^{\circ} - \Delta G_{ads}^{\circ}}{T} \quad (19)$$

**Table 6: Temkin parameters at temperature range 20 – 60 °C**

Temp. °C	R <sup>2</sup>	<i>a</i>	$K_{ads}$ mol <sup>-1</sup>	$\Delta G_{ads}^{\circ}$ kJ/mol	$\Delta H_{ads}^{\circ}$ kJ/mol	$\Delta S_{ads}^{\circ}$ J/mol K
20	0.9672	-10.0	1.08E+07	-49.2	303.577	1.20
30	0.9180	-14.6	4.74E+10	-72.0		1.24
40	0.9180	-15.2	1.94E+11	-78.1	or	1.22
50	0.8996	-14.1	3.26E+10	-75.8		1.17
60	0.7736	-19.9	1.81E+15	-108.4	303.580	1.23

As shown in Table 6, the adsorptive equilibrium constant ( $K_{ads}$ ) generally increased with increasing of temperature. This indicated that adsorption of END on the Sn surface was favorable at higher temperatures. Generally, larger

values of  $K_{ads}$  is bound up with more efficient adsorption and hence better inhibition efficiency of a given inhibitor (Singh and Quraishi, 2011; Ansari *et al.*, 2014 and Ejikeme *et al.*, 2015).

Values of  $\Delta G_{ads}^{\circ}$  were more negative than -40 kJ/mol meaning that adsorption process was spontaneous (AL-Sawaad, 2013) and involved charge sharing or transfer from the inhibitor's molecule to the metal surface leading to the formation of a donor-acceptor bond (chemical adsorption) (Eddy *et al.*, 2010). It has been commonly recognized that an organic inhibitor usually promotes formation of a chelate on a metal surface by electron transfer from the organic compound to the metal and form a coordinate covalent bond during the chemical adsorption (Fouda *et al.*, 2015). In this type of adsorption, the metal (Sn) acts as an electrophile while the inhibitor (END) acts as a nucleophile (Fang and Li, 2002 and Eddy *et al.*, 2010).

The positive  $\Delta H_{ads}^{\circ}$  values indicated that the degree of surface coverage increased with rise in temperature (Obot *et al.*, 2011). This supported the earlier proposed mechanism of chemical adsorption for END on Sn surface.

The positive values of  $\Delta S_{ads}^{\circ}$  in the presence of inhibitor could be attributed to the increase in the solvent entropy and more positive desorption entropy. It was also interpreted that the increase of disorderness was due to more water molecules which could be desorbed from the metal surface by one inhibitor molecule (Bhat and Alva, 2011).

Hence, according to the above results, corrosion inhibition of Sn by END is assumed to occur primarily through chemical adsorption, giving rise to the activation of the surface to hydrogen atom recombination. Similar results have been reported in earlier publications (Umoren and Obot, 2008; Ekanem *et al.*, 2010 and Obot *et al.*, 2011).

### Conclusions:-

Expired Novacid drug (END) showed excellent inhibition performance for tin corrosion in 1M HCl solution. The inhibition efficiencies, obtained from weight loss and potentiodynamic polarization measurements, increased with increasing both concentration of END and temperature of solution. The results of weight loss measurements, illustrated that the inhibition process followed first-order kinetics at all studied concentrations and temperatures. From polarization measurements, END showed excellent inhibition performance as a cathodic-type inhibitor for tin corrosion in 1M HCl solution. The adsorption of END followed the Temkin's adsorption isotherm. Gibbs free energy, enthalpy and entropy of adsorption, all indicated that the process of adsorption was spontaneous and exothermic and the molecules adsorbed to the metal surface by chemical adsorption. Positive values of enthalpy of activation reflected the endothermic nature of tin dissolution process. While negative values of entropy of activation indicated the increase in the system ordering.

### References:-

1. Abd El-Rehim, S.S., Hassan, H.H. and Mohamed, N.F. (2004): Anodic behaviour of tin in maleic acid solution and the effect of some inorganic inhibitors. *Corros. Sci.*, **46**: 1071–1082.
2. Abd El-Rehim, S.S., Zaky, A.M. and Mohamed, N.F. (2006): Electrochemical behaviour of a tin electrode in tartaric acid solutions. *J. Alloys Compd.*, **424(1)**: 88– 92.
3. Abdel Motaal, S.M. and AL-Malki, H.A. (2009): Corrosion inhibition of Al-Cu alloy in acidic media by Cassia Acutifolia extract. *Al-Azhar Bull. Sci.*, **20(2)**: 89–105.
4. Al-Bonayan, A.M. (2015): Corrosion inhibition of carbon steel in hydrochloric acid solution by Senna-Italica extract. *IJRRAS.*, **22(2)**: 49– 64.
5. AL-Sawaad, H.Z. (2013): Evaluation of the ceftriaxone as corrosion inhibitor for carbon steel alloy in 0.5M of hydrochloric acid. *Int. J. Electrochem. Sci.*, **8**: 3105– 3120.
6. Ansari, A., Znini, M., Hamdani, I., Majidi, L., Bouyanzer, A. and Hammouti, B. (2014): Experimental and theoretical investigations anti-corrosive properties of Menthone on mild steel corrosion in hydrochloric acid. *J. Mater. Environ. Sci.*, **5(1)**: 81– 94.
7. Artander, S. (1969): Perfume and Flavour chemicals (Aroma chemicals) II. No. 2053. Montclair, New York.
8. Atkins, P. and Paula, J.d. (2014): Atkins' Physical Chemistry. 10<sup>th</sup> Ed., Oxford: Oxford Press.
9. Attia, E.M. (2015): Expired Farcolin drug as corrosion inhibitor for carbon steel in 1M HCl solution. *J. Basic. Appl. Chem.*, **5(1)**: 1–15.
10. Bhat, J.I. and Alva, V.D.P. (2011): Meclizine hydrochloride as a potential non-toxic corrosion inhibitor for mild steel in hydrochloric acid medium. *Arch. Appl. Sci. Res.*, **3(1)**: 343–356.

11. Bockris, J.O.M. and Reddy, A.K.N. (2000): *Modern Electrochemistry 2B, Electrode processes in chemistry, engineering, biology and environmental science*. 2<sup>nd</sup> Ed., Kluwer Academic/Plenum Publishers, New York.
12. Cotton, F.A. and Wilkinson, G. (1972): *Advanced Inorganic Chemistry*. 3<sup>rd</sup> Ed., Interscience-Wiley, New York.
13. Eddy, N.O., Stoyanov, S.R. and Ebenso, E.E. (2010): Fluoroquinolones as corrosion inhibitors for mild steel in acidic medium; experimental and theoretical studies. *Int. J. Electrochem. Sci.*, **5**: 1127– 1150.
14. Ejikeme, P. M., Umana, S.G., Menkiti, M.C. and Onukwuli, O.D. (2015): Inhibition of mild steel and aluminium corrosion in 1M H<sub>2</sub>SO<sub>4</sub> by leaves extract of African Breadfruit. *Int. J. Mat.Chem.*, **5**(1): 14–23.
15. Ekanem, U.F., Umoren, S.A., Udousoro, I.I. and Udoh, A.P. (2010): Inhibition of mild steel corrosion in HCl using pineapple leaves (*Ananas comosus* L.) extract. *J. Mat. Sci.*, **45**(20): 5558– 5566.
16. El-Sherif, R.M. and Badawy, W.A. (2011): Mechanism of corrosion and corrosion inhibition of tin in aqueous solutions containing tartaric acid. *Int. J. Electrochem. Sci.*, **6**: 6469– 6482.
17. Fang, J. and Li, J. (2002): Quantum chemistry study on the relationship between molecular structure and corrosion inhibition efficiency of amides. *J. Mol. Struct. (Theochem)*, **593**: 179– 185.
18. Fouda, A.S., Abdel-Maksoud, S.A. and Almetwally, A.E. (2015): Corrosion inhibition of tin in sodium chloride solutions using propaneitrile derivatives. *Chem. Sci. Trans.*, **4**(1): 161–175.
19. Golestani, Gh., Shahidi, M. and Ghazanfari, D. (2014): Electrochemical evaluation of antibacterial drugs as environment-friendly inhibitors for corrosion of carbon steel in HCl solution. *Appl. Surf. Sci.*, **308**: 347–362.
20. Hassan, H. H. and Fahmy, K. (2008): Pitting corrosion of tin by acetate anion in acidic media. *Int. J. Electrochem. Sci.*, **3**: 29– 43.
21. Karthik, R., Muthukrishnan, P., Chen, S.M., Jeyaprabha, B. and Prakash, P. (2015): Anti-corrosion inhibition of mild steel in 1M hydrochloric acid solution by using *Tiliacora acuminate* leaves extract. *Int. J. Electrochem. Sci.*, **10**: 3707– 3725.
22. Lokesh, H.B., Fakrudeen, S.P. and Bheema Raju, V.B. (2014): An electrochemical investigation on the corrosion behavior of ZA-27 alloy in 1M Na<sub>2</sub>SO<sub>4</sub> in the presence of cationic surfactants as inhibitors. *IOSR-JHSS.*, **19**(6): 9–20.
23. Lyon, S.B. (2010): *Corrosion of tin and its alloys*. Shreir's Corrosion, T. J. A. Richard- son, Ed., Elsevier, New York, 2068–2077.
24. Mohran, H.S., El-Sayed, A. and Abd El-Lateef, H.M. (2009): Anodic behavior of tin, indium, and tin–indium alloys in oxalic acid solution. *J. Sol. St. El.*, **13**(8): 1279–1290.
25. Obot, I.B., Umoren S.A and Obi-Egbedi, N.O. (2011): Corrosion inhibition and adsorption behaviour for aluminum by extract of *Aningeria robusta* in HCl solution: Synergistic effect of iodide ions. *J. Mater. Environ. Sci.*, **2**(1): 60–71.
26. Pardo, A., Merino, M.C., Carboneras, M., Viejo, F., Arrabal, R. and Muñoz, J. (2006): Influence of Cu and Sn content in the corrosion of AISI 304 and 316 stainless steels in H<sub>2</sub>SO<sub>4</sub>. *Corros. Sci.*, **48**(5): 1075–1092.
27. Pathak, R.K. (2013): Electrosynthesis and characterization of CdSeHgTl thin films. *RJCS.*, **3**(4): 44–47.
28. Sharma, K.K. and Sharma, L.K. (2008): *A textbook of physical chemistry*. 4<sup>th</sup> Ed., Vikas Pub. House, Vedams eBooks (P) Ltd (New Delhi, India).
29. Sharma, S.K., Peter, A. and Obot, I.B. (2015): Potential of *Azadirachta indica* as a green corrosion inhibitor against mild steel, aluminum, and tin: a review. *JAST.*, **6**(26): 1–16.
30. Sheeja, V.N. and Subhashini, S. (2014): Pavetta Indica Bark as corrosion inhibitor in mild steel corrosion in HCl and H<sub>2</sub>SO<sub>4</sub> medium: Adsorption and thermodynamic study. *Chem. Sci. Trans.*, **3**(1): 129–140.
31. Sığircık, G., Tüken, T. and Erbil, M. (2016): Assessment of the inhibition efficiency of 3,4-diaminobenzonitrile against the corrosion of steel. *Corros. Sci.*, **102**: 437– 445.
32. Singh, A.K. and Quraishi, M.A. (2011): Adsorption properties and inhibition of mild steel corrosion in hydrochloric acid solution by ceftobiprole. *J. Appl. Electrochem.*, **41**(1): 7–18.
33. Smith, A.E. (1973): A study of the variation with pH of the solubility and stability of some metal ions at low concentrations in aqueous solution. Part I. *Analyst*, **98**: 209– 212.
34. Szauer, T. and Brand, A. (1981): Mechanism of inhibition of electrode reactions at high surface coverages-II. *Electrochim. Acta.*, **26**(9): 1219– 1224.
35. Umoren, S.A. and Obot, I.B. (2008): Polyvinylpyrrolidone and polyacrylamide as corrosion inhibitors for mild steel in acidic medium. *Surf. Rev. Let.*, **15**(3): 277– 286.
36. Zhang, D., Tang, Y., Qi, S., Dong, D., Cang H. and Lu, G. (2016): The inhibition performance of long-chain alkyl-substituted benzimidazole derivatives for corrosion of mild steel in HCl. *Corros. Sci.*, **102**: 517–522.
37. Zhu, Y., Free, M.L. and Yi, G. (2016): The effects of surfactant concentration, adsorption, aggregation, and solution conditions on steel corrosion inhibition and associated modeling in aqueous media. *Corros. Sci.*, **102**: 233–250.